COMMUNICATION

Excitonic Properties and Near-Infrared Coherent Random Lasing in Vertically Aligned CdSe Nanowires

Rui Chen, Muhammad Iqbal Bakti Utama, Zeping Peng, Bo Peng, Qihua Xiong, and Handong Sun**

One-dimensional (1D) semiconductor nanowires (NWs) have drawn considerable research attention over the past few decades because of their unique properties and potential applications in nanoelectronics, photonics, luminescent materials, lasing materials, and biological and medical sensing.[1–3] Impressive progress has been demonstrated in highly efficient light sources (nanolasers), waveguides, field-effect transistors and photodetectors based on group IV elements (Si and Ge),[4] III–V compound semiconductors (GaN and GaAs),[2,5] and semiconducting oxides (ZnO, SnO_2 and In_2O_3).[6,7] Owing to its direct bandgap (ca. 1.74 eV at room temperature), good absorption ability, and excellent photosensitivity,[8,9] CdSe is recognized as a promising light-harvesting material to be applied in optoelectronics. Especially, the fundamental emission of CdSe falls in the near-infrared (NIR) region, and biosensors operating in this region can avoid interference from biological media such as tissue autofluorescence and scattering light, and thereby facilitate relatively interference-free sensing.[10]

At present, studies on CdSe-based materials are extensively focused on colloidal CdSe quantum dots (QDs).[11] Varying the size of the nanocrystals allows the bandgap of CdSe QDs to be tuned to cover the whole visible region up to the NIR region. However, colloidal QDs form clusters easily, and some special ligands need to be added for dispersion. Thus, colloidal QDs may not be very stable under ultraviolet (UV) radiation.[12] In comparison, CdSe NWs can circumvent this drawback, because very high crystalline quality can be readily achieved through the vapor–solid–liquid (VLS) growth mechanism. Nevertheless, only very few papers have reported the synthesis of 1D CdSe NWs.[8,9,13–16] Descriptions of detailed investigations of the intrinsic optical properties of CdSe NWs, in order to assess their possible applications, are still unavailable.[17]

In the study reported here, high-quality CdSe NW arrays were obtained through a vapor-transport growth technique. The excitonic optical properties were investigated systematically by measurements of optical absorption and photoluminescence (PL) down to 10 K. We observed a very sharp exciton absorption peak and narrow PL. The Stokes shift is as small as 1.3 meV, indicating high crystalline quality. By means of optical pumping with a pulsed green laser, we observed NIR coherent random lasing from CdSe NWs at room temperature for the first time, which evidences high optical gain, stemming from the high crystalline quality, suggesting significant potential for applications in optoelectronics.

Figure 1a shows a scanning electron microscopy (SEM) image of the as-grown array sample, displaying a high-density array of vertically aligned CdSe NWs. The diameter of CdSe nanowires is ca. 70 nm and follows the log-normal distribution. A detailed description of the sample synthesis based on a van der Waals growth mechanism and the characterization can be found elsewhere.[18] A high-resolution transmission electron microscopy (TEM) image of a single CdSe NW is given in Figure 1b. The measured lattice spacing and the growth direction of the wurtzite-type NW are indicated. The NW possessed an obtuse-angled tip in place of the metal catalyst usually found in NWs grown using the conventional VLS technique. The good single crystallinity of the sample can be readily inspected from the well-defined lattice fringes and the clear selected-area electron diffraction (SAED) pattern shown in the inset of Figure 1b.

Figure 2a shows the absorption spectra of CdSe NWs obtained at 10 K, while the temperature-dependent absorption mapping is drawn in Figure 2b. It can be seen that strong excitonic features dominate the low temperature spectra. The sharp absorption peak located at 1.8248 eV can be ascribed to the free-exciton absorption (FX_A) of CdSe. In the higher energy part of the absorption spectra, another peak can be observed at 1.8515 eV. The energy difference between this peak and FX_A is ca. 26.68 meV, which coincides with the longitudinal optical (LO) phonon energy of CdSe,[19] and thus can be denoted as FX_A+1LO. If the continuous background introduced by the absorption edge is subtracted, the spectrum can be well fitted by a multi-Gaussian equation. The evolution of the absorption features with temperature can be clearly seen from the mapping. The shifts of the exciton absorption peak and its phonon replica as a function of temperature display conventional bandgap shrinkage, which is due to both thermal expansion and exciton–phonon interaction. The overall contribution to the shift can be described by the Bose–Einstein approximation[20]

$$E(T) = E(0) - 2\alpha_B[\exp(\theta/T) - 1]^{-1} \quad (1)$$

where $E(0)$ is the exciton energy at $T = 0$ K, α_B is the strength of the average electron–phonon interaction, $[\exp(\theta/T)-1]^{-1}$ is the Bose–Einstein statistical factor for phonon absorption,

R. Chen, M. I. B. Utama, Z. P. Peng, B. Peng,
Prof. Q. H. Xiong, Prof. H. D. Sun
Division of Physics and Applied Physics
School of Physical and Mathematical Sciences
Nanyang Technological University
Singapore 637371, Singapore
E-mail: qihua@ntu.edu.sg; hdsun@ntu.edu.sg
Prof. Q. H. Xiong
Division of Microelectronics
School of Electrical and Electronics Engineering
Nanyang Technological University
Singapore 639798, Singapore

DOI: 10.1002/adma.201003820

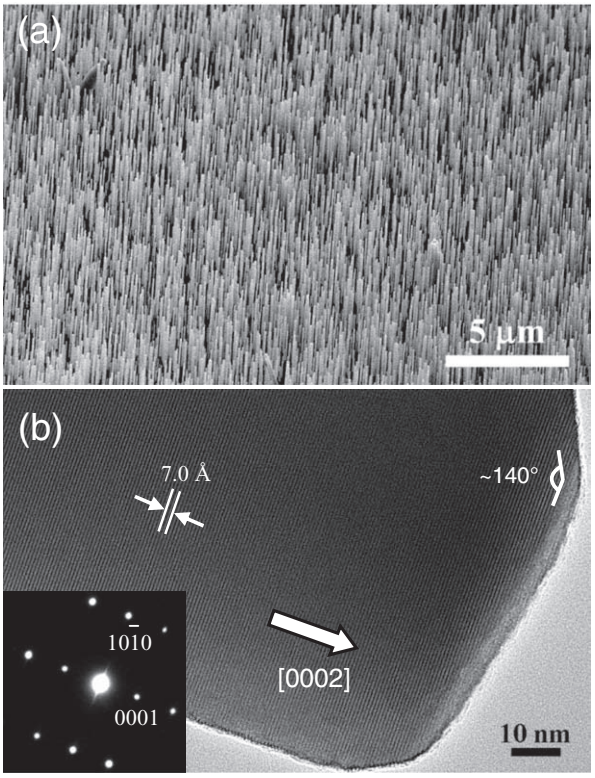

Figure 1. a) SEM image of the as-grown CdSe NWs. b) High-resolution TEM image of an individual CdSe NW. The inset shows a SAED pattern from the same NW.

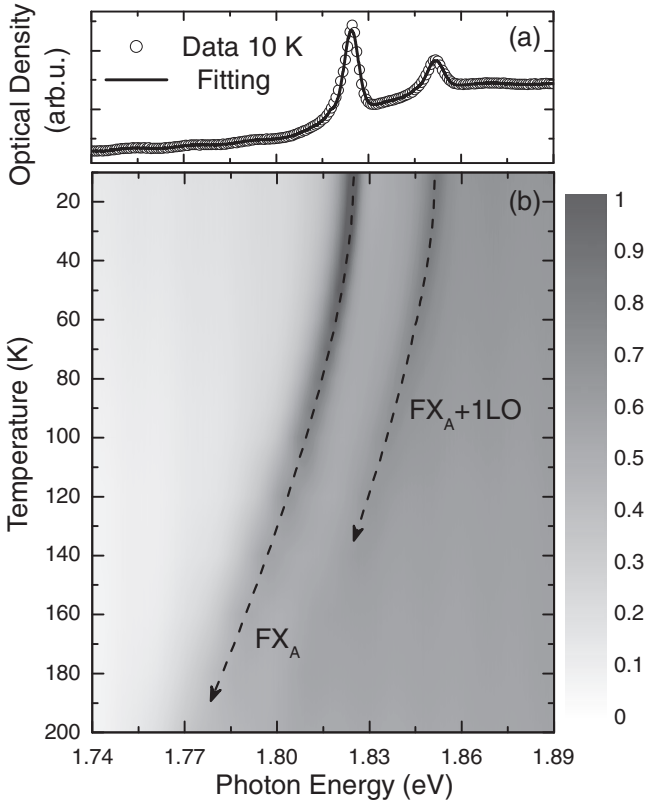

Figure 2. a) Low temperature (10 K) free-exciton absorption of CdSe NWs. The solid curve is the multi-Gaussian fitting of the absorption spectrum. b) Temperature-dependent mapping of the absorption spectrum.

and θ is the temperature corresponding to the average phonon energy. As shown in **Figure 3**a, the evolution of the absorption peak FX_A can be well fitted by Equation 1. Then the curve is vertically shifted by 26.68 meV for FX_A+1LO. The fitting parameters obtained are $E(0)$ = 1.824 eV, α_B = 27 meV, and θ = 151 K. The average phonon temperature θ in the sample is lower than the LO phonon temperature (ca. 310 K), which indicates the larger contribution of the acoustic phonons to the bandgap shrinkage. Taking the bulk CdSe exciton binding energy (15.0 meV) into account,[21] the values of the fundamental bandgap deduced from our measurements are 1.756 eV at room temperature and 1.839 eV at 10 K, which is in agreement with the reported data.[22–24]

The temperature-dependent excitonic broadening can provide us with information about the exciton–phonon interaction. As is well known, the exciton linewidth broadening originates from two contributions: the inhomogeneous broadening due to impurities and crystal imperfections, and the homogeneous broadening due to acoustic-phonon and LO-phonon scatterings.[22] Based on the above discussion, the temperature dependence of the full width at half maximum (FWHM) can be approximately described by[25,26]

$$\Gamma(T) = \Gamma_{inh} + \Gamma_h = \Gamma_{inh} + \gamma_{ph} T + \frac{\Gamma_{LO}}{\left[\exp\left(\hbar\omega_{LO}/k_B T\right) - 1\right]} \qquad (2)$$

where Γ_{inh} and Γ_h are the inhomogeneous and homogenous contributions, respectively. ν_{ph} is the coupling strength of the exciton–acoustic phonon interaction, Γ_{LO} is the coupling strength of the exciton–LO phonon interaction, and $\hbar\omega_{LO}$ = 26.68 meV is the LO-phonon energy. We find the fit to be excellent with the parameters Γ_{inh} = 4.748 meV, ν_{ph} = 25.96 μeV K^{-1}, and Γ_{LO} = 44.41 meV. In Figure 3b, the dashed line shows the contribution from acoustic-phonon scattering, while the dash-dotted line shows the contribution from the LO phonons. It is noticeable that the acoustic phonons contribute up to 70 K very significantly. From 70 K onward, due to the increase of phonon population, the participation of LO phonons causes the FWHM to increase sharply. At 110 K, there is a crossover and the LO phonons dominate over the acoustic phonons. The strength of the exciton–LO phonon interaction is an important parameter since it affects optical and electrical properties of semiconductors (emission line broadening, hot carrier cooling, and carrier mobility). Therefore, it is interesting to compare the value with those in other wide-bandgap semiconductors. The value of Γ_{LO} is comparable to that of II-S (ZnS: 40.78 meV[27] and CdS: 41 meV[28]), but significantly smaller than the values reported for oxides (ZnO: 876 meV)[29] and nitrides (GaN: 525 meV).[26] It is found that the strength of electon–phonon coupling is related to LO-phonon energy. Wurtzite-type CdSe possesses phonon energy of 26.68 meV, which is comparable to that of ZnS (42.95 meV)[30] and CdS (38 meV), but smaller than that of ZnO (72 meV) and GaN (92 meV).[22] Therefore, we expect that the performance of devices based on CdSe at high temperature,

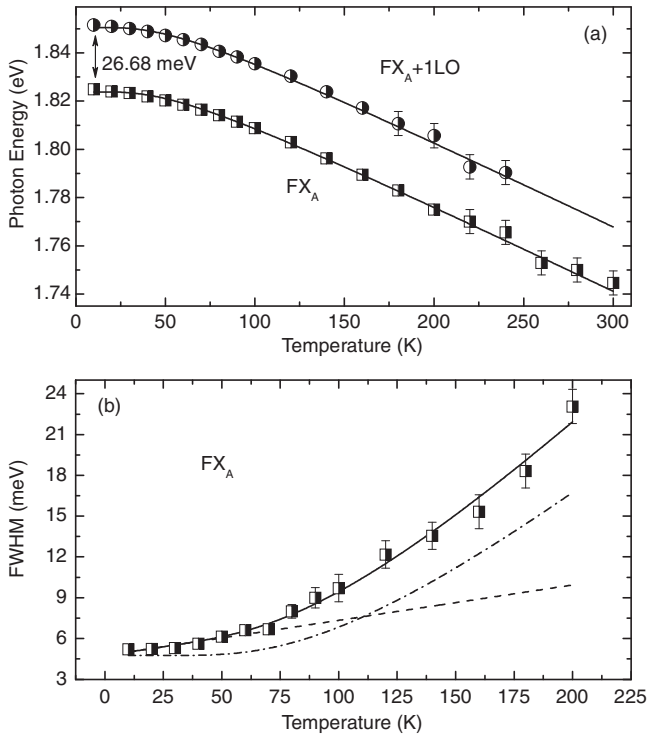

Figure 3. a) The temperature dependence of the free-exciton-absorption peak energy with its first-order LO phonon absorption. The solid line is the fitting based on Equation 1 and then shifted vertically by 26.68 meV. b) Temperature dependence of the FWHM of the free-exciton absorption. The solid curve is the fitting based on Equation 2. The dashed line shows the contribution from the acoustic-phonon scattering alone, and the dash-dotted line indicates the contribution from the LO phonon only. In both cases inhomogeneous broadening was added.

as compared to ZnO- and GaN-based devices, will be significantly less affected by the exciton–LO phonon interaction.

Figure 4 depicts the low temperature (10 K) PL spectrum of CdSe NWs under laser excitation at 325 nm (1 mW) with a spot ca. 1 mm^2 in area. The intensity of longer wavelength emission is multiplied by a factor of 10 for clarity. The broad emission (ca. 1.53 eV) may come from impurities or structural defects formed during the material growth, which will not be discussed here. As shown in Figure 4, the emission at ca. 1.824 eV is the bandgap emission of CdSe NWs, and is denoted as free-exciton emission (FX_E). The linewidth of the emission is only ca. 8.4 meV. Compared to the FX_A, the Stokes shift (Δ_{ss}) is deduced to be only 1.3 meV. The small value of Δ_{ss} obtained in our CdSe NWs relative to other reported data[31,32] indicates the high crystalline quality of the NWs, which also accounts for the weak intensity of the deep level emission. The integrated PL intensity of FX_E under different excitation densities is shown in the inset of Figure 4. The PL intensity (I_{PL}) can be expressed as a function of the excitation laser power (I_{EX}) as $I_{PL} \propto I_{EX}^{\alpha}$, where α is the nonlinear exponent.[33] It can be seen that the integrated PL intensity of CdSe NWs increases approximately linearly with the excitation density. By fitting the experimental data, a value of ca. 1.1 for the nonlinear exponent α is obtained, which supports the free-excitonic nature of the emission from CdSe NWs.

Next, we examined the temperature dependence of the PL emission from CdSe NWs. As can be seen in **Figure 5**, a gradual decrease in the PL intensity with increasing temperature can be observed. In fact, the temperature-dependent integrated PL intensity is not well reproduced by an Arrhenius plot with a single thermal activation. However, it can be adequately described by the following dual activation energy model:[34]

$$I(T) = \frac{I(0)}{1 + c_1 \exp\left(-E_1/k_B T\right) + c_2 \exp\left(-E_2/k_B T\right)} \quad (3)$$

where E_1 and E_2 denote different activation energies for two different thermal activation processes, and the parameters c_1 and c_2 are the relative ratios of nonradiative recombination. From a least squares fitting procedure using Equation 3, the activation energies obtained are estimated to be 5.40 and

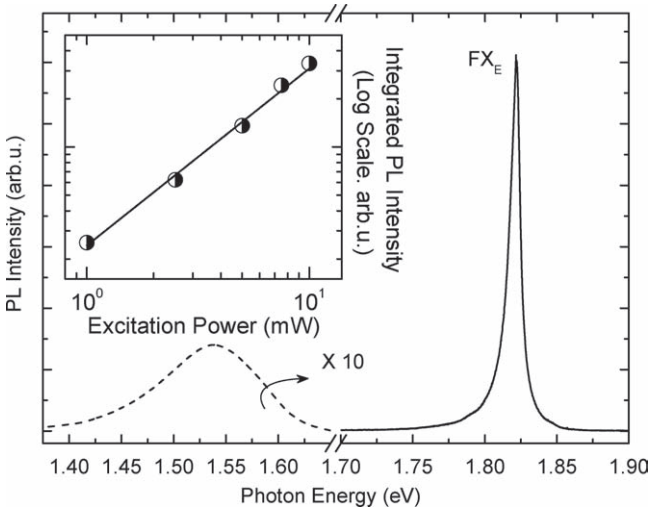

Figure 4. Low-temperature (10 K) PL spectrum of CdSe NWs under laser (325 nm) excitation. The inset shows the integrated PL intensity for different excitation powers.

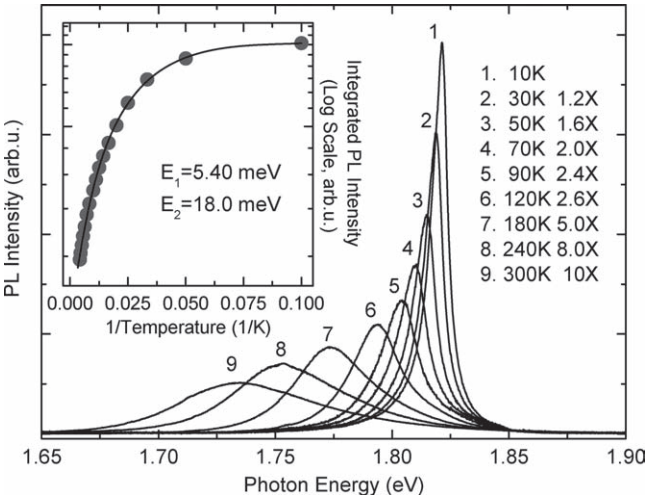

Figure 5. The free-exciton emission of CdSe NWs at various temperatures. The inset plots the dependence of the integrated PL intensity on the reciprocal of temperature, and the solid curve is the Arrhenius fit with two activation energies.

18.0 meV, respectively. The former activation energy is small and may be related to the thermally activated capture of excitons by nonradiative defects in CdSe,[35] while the latter one corresponds to the thermal energy required for the dissociation of free excitons into the continuum states. It is noted that the obtained activation energy (18.0 meV) is comparable to the exciton binding energy of bulk CdSe (15.0 meV), which supports our assignment.[21]

We have examined the emission characteristics of the sample under high power density excitation through a pulsed laser. **Figure 6**a shows the PL spectra of CdSe NWs under different excitation densities at room temperature. The sample displayed a weak spontaneous emission under low excitation of ca. 0.137 MW cm^{-2}. When the excitation density exceeds a threshold of 0.296 MW cm^{-2}, sharp peaks with a linewidth as narrow as 0.4 nm emerge from the broad spontaneous emission spectrum, indicating the appearance of lasing action. As the excitation density increases, multiple spikes between 715 and 725 nm can be detected. A plot of integrated PL intensity of these stimulated peaks with respect to excitation density is given in the inset of Figure 6a.

One may try to relate the lasing to a Fabry–Pérot (F-P) cavity, in which the light is confined between two end facets of one single CdSe NW.[1] However, the refractive index of CdSe at ca. 720 nm is 2.4,[36] and thus the F-P modes suffer strongly from mirror losses at the CdSe/air interface, owing to a low reflectivity of about 17%. Moreover, the tip of the CdSe NW possesses an obtuse angle, which will introduce very strong optical losses. So it is considered that F-P lasing action is difficult in our CdSe NWs.

As plotted in Figure 6b, it is clearly seen that different emission spectra were recorded in different directions. These characteristics of the emission are qualitatively consistent with random lasing behavior with coherent feedback.[37] It is worth mentioning that most random lasing has only been observed in the UV wavelength range in oxide materials, which have high exciton oscillation strength: initially in ZnO nanoparticles[37] and recently in SnO_2.[38] The observation of NIR lasing

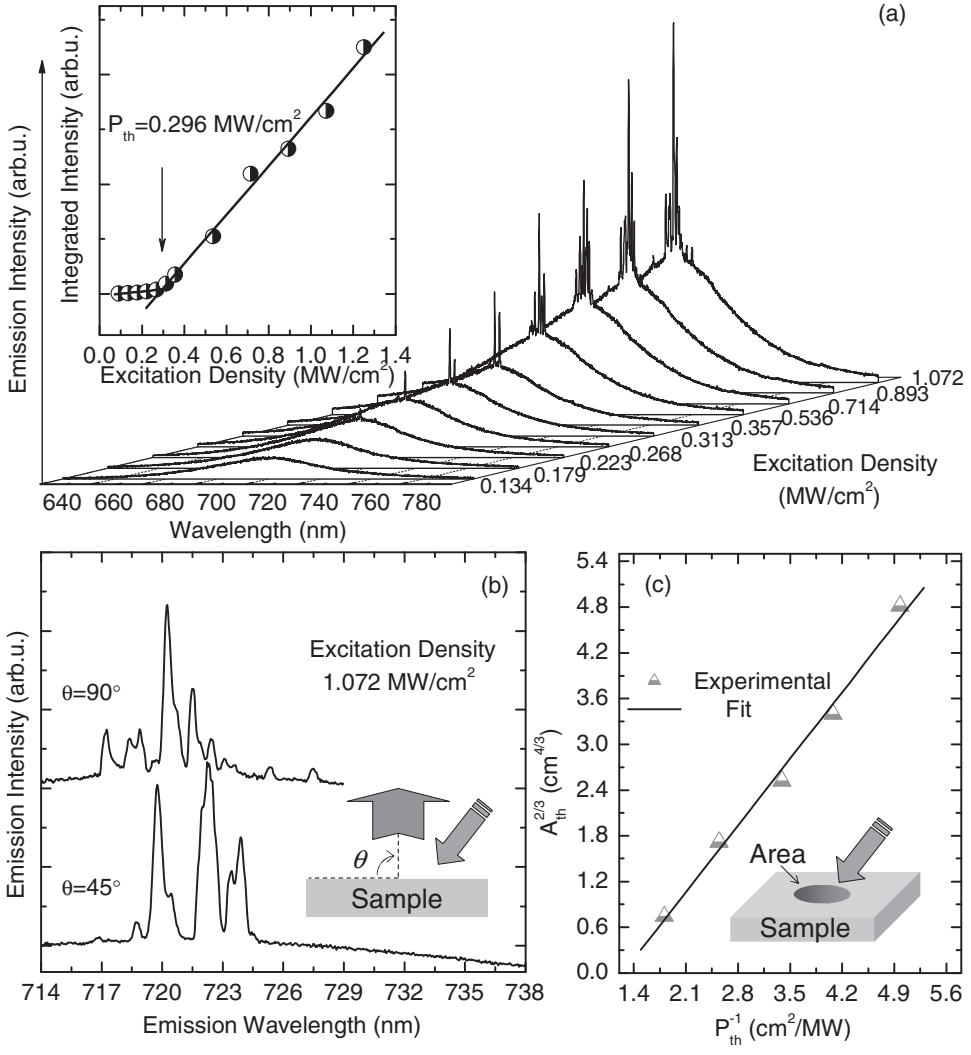

Figure 6. a) The emission spectra from CdSe NWs at room temperature under different excitation densities. The inset shows the dependence of the PL integrated intensity on the laser excitation density. b) Emission spectra of CdSe NWs detected at two different observation angles. c) The random lasing threshold of CdSe NWs for different excitation areas.

from CdSe NWs can be ascribed to the high quality and thus high optical gain of our sample, which point toward potential optoelectronic applications of this material system.

The dependence of excitation area (A_{th}) on the random lasing threshold (P_{th}) under constant pump power was also studied and the data is presented in Figure 6c. When the excitation area is increased, the pump threshold needed to create random lasing decreases. Coherent random laser theory indicates that in three dimensions the pump area and pump threshold can be related by $A_{th}^{2/3} \approx K P_{th}^{-1}$, where K is a constant.[39,40] It is found that experimental data is well satisfied by this relationship. In this case, the vertically aligned CdSe NWs should behave like a quasi-3D random medium. This again proves that coherent random laser action exists in our samples.

In conclusion, we have reported systematic investigations of high-quality arrays of vertically aligned CdSe NWs. Strong free-exciton absorption and emission were observed and analyzed at low temperature. Based on the analysis of temperature-dependent optical properties, it is shown that CdSe NW material is significantly less affected by the exciton–LO phonon interaction compared to ZnO and GaN, which may result in improved high-temperature performance of devices based on CdSe. Moreover, the high-quality CdSe NWs show intense NIR lasing peaks under optical excitation at room temperature. Such lasing emissions are identified as multimode random lasing, which is correlated with the 3D arrangement of the CdSe NWs. Our investigations demonstrate the unique optical properties of CdSe NWs, which might be useful for NIR optoelectronic device applications such as lasers, sensors, and solar energy conversion devices.

Experimental Section

The CdSe NWs used in this investigation were grown by the self-catalytic vapor transport approach with van der Waals epitaxy on (001) muscovite mica substrate.[18] A JEOL JSM-7001F field emission scanning electron microscope and a JEOL JEM-2100 transmission electron microscope were used to characterize the morphology of the sample. The absorption measurements of the sample were performed between 10 and 300 K within a helium closed-cycle cryostat. A 250 W tungsten halogen lamp was used as the light source and the signal was dispersed by a 0.75 m monochromator combined with suitable filters, and detected by a charge-coupled device (CCD). A He-Cd laser with laser line of 325 nm was used as the excitation source during PL measurement. For lasing demonstration, the signal was detected using the same system, except that the excitation source was replaced by a pulsed Nd:YAG second-harmonic (532 nm) laser. The pulse width and repetition rate of the laser were about 1 ns and 60 Hz, respectively.

Acknowledgements

Support from the Singapore Ministry of Education through the Academic Research Fund (Tier 1) under Project No. RG40/07 and from Singapore National Research Foundation through a NRF fellowship grant (NRF-RF2009 – 06), and a generous start-up grant (M58110061) from Nanyang Technological University are gratefully acknowledged.

Received: October 16, 2010
Published online: February 15, 2011

[1] M. H. Huang, S. Mao, H. Feick, H. Yan, Y. Wu, H. Kind, E. Weber, R. Russo, P. Yang, *Science* **2001**, *292*, 1897.
[2] X. Duan, Y. Huang, R. Agarwal, C. M. Lieber, *Nature* **2003**, *421*, 241.
[3] X. Wang, C. J. Summers, Z. L. Wang, *Nano Lett.* **2004**, *4*, 423.
[4] J. Xiang, W. Lu, Y. Hu, Y. Wu, H. Yan, C. M. Lieber, *Nature* **2006**, *441*, 489.
[5] J. Zhou, Y. Gu, P. Fei, W. Mai, Y. Gao, R. Yang, G. Bao, Z. L. Wang, *Nano Lett.* **2008**, *8*, 3035.
[6] M. Law, L. E. Greene, J. C. Johnson, R. Saykally, P. Yang, *Nat. Mater.* **2005**, *4*, 455.
[7] R. Chen, G. Z. Xing, J. Gao, Z. Zhang, T. Wu, H. D. Sun, *Appl. Phys. Lett.* **2009**, *95*, 061908.
[8] C. Ma, Z. L. Wang, *Adv. Mater.* **2005**, *17*, 2635.
[9] G. X. Wang, M. S. Park, H. K. Liu, D. Wexler, J. Chen, *Appl. Phys. Lett.* **2006**, *88*, 193115.
[10] Y. Zhang, Y. Li, X.-P. Yan, *Anal. Chem.* **2009**, *81*, 5001.
[11] C. B. Murray, D. J. Norris, M. G. Bawendi, *J. Am. Chem. Soc.* **1993**, *115*, 8706.
[12] M. Jones, J. Nedeljkovic, R. J. Ellingson, A. J. Nozik, G. Rumbles, *J. Phys. Chem. B* **2003**, *107*, 11346.
[13] Z. Li, Ö. Kurtulus, N. Fu, Z. Wang, A. Kornowski, U. Pietsch, A. Mews, *Adv. Funct. Mater.* **2009**, *19*, 3650.
[14] N. Shpaisman, U. Givan, F. Patolsky, *ACS Nano* **2010**, *4*, 1901.
[15] Z. Feng, Q. Zhang, L. Lin, H. Guo, J. Zhou, Z. Lin, *Chem. Mater.* **2010**, *22*, 2705.
[16] D. Xu, X. Shi, G. Guo, L. Gui, Y. Tang, *J. Phys. Chem. B* **2000**, *104*, 5061.
[17] C. Ma, Y. Ding, D. Moore, X. Wang, Z. L. Wang, *J. Am. Chem. Soc.* **2004**, *126*, 708.
[18] M. I. B. Utama, Z. Peng, R. Chen, B. Peng, X. Xu, Y. Dong, L. M. Wong, S. J. Wang, H. D. Sun, Q. Xiong, *Nano Lett.*, DOI: 10.1021/nl1034495.
[19] L. Biadala, Y. Louyer, P. Tamarat, B. Lounis, *Phys. Rev. Lett.* **2009**, *103*, 037404.
[20] P. Lautenschlager, M. Garriga, S. Logothetidis, M. Cardona, *Phys. Rev. B* **1987**, *35*, 9174.
[21] G. D. Scholes, G. Rumbles, *Nat. Mater.* **2006**, *5*, 683.
[22] C. H. Chia, C. T. Yuan, J. T. Ku, S. L. Yang, W. C. Chou, J. Y. Juang, S. Y. Hsieh, K. C. Chiu, J. S. Hsu, S. Y. Jeng, *J. Lumin.* **2008**, *128*, 123.
[23] S. Ninomiya, S. Adachi, *J. Appl. Phys.* **1995**, *78*, 4681.
[24] R. G. Wheeler, J. O. Dimmock, *Phys. Rev.* **1962**, *125*, 1805.
[25] H. D. Sun, T. Makino, N. T. Tuan, Y. Segawa, M. Kawasaki, A. Ohtomo, K. Tamura, H. Koinuma, *Appl. Phys. Lett.* **2001**, *78*, 2464.
[26] A. K. Viswanath, J. I. Lee, D. Kim, C. R. Lee, J. Y. Leem, *Phys. Rev. B* **1998**, *58*, 16333.
[27] R. Chen, D. Li, B. Liu, Z. Peng, G. G. Gurzadyan, Q. Xiong, H. D. Sun, *Nano Lett.* **2010**, *10*, 49560.
[28] S. Rudin, T. L. Reinecke, B. Segall, *Phys. Rev. B* **1990**, *42*, 11218.
[29] T. Makino, C. H. Chia, N. T. Tuan, Y. Segawa, M. Kawasaki, A. Ohtomo, K. Tamura, H. Koinuma, *Appl. Phys. Lett.* **2000**, *76*, 3549.
[30] Q. Xiong, G. Chen, J. D. Acord, X. Liu, J. J. Zengel, H. R. Gutierrez, J. M. Redwing, L. C. Lew Yan Voon, B. Lassen, P. C. Eklund, *Nano Lett.* **2004**, *4*, 1663.
[31] P. Nandakumar, C. Vijayan, Y. V. G. S. Murti, *J. Appl. Phys.* **2002**, *91*, 1509.
[32] T. J. Liptay, L. F. Marshall, P. S. Rao, R. J. Ram, M. G. Bawendi, *Phys. Rev. B* **2007**, *76*, 155314.
[33] L. Bergman, X.-B. Chen, J. L. Morrison, J. Huso, A. P. Purdy, *J. Appl. Phys.* **2004**, *96*, 675.
[34] H. D. Sun, S. Calvez, M. D. Dawson, J. A. Gupta, G. C. Aers, G. I. Sproule, *Appl. Phys. Lett.* **2006**, *89*, 101909.
[35] R. Chen, Y. Y. Tay, J. Ye, Y. Zhao, G. Z. Xing, T. Wu, H. D. Sun, *J. Phys. Chem. C* **2010**, *114*, 17889.
[36] B. Jensen, A. Torabi, *J. Opt. Soc. Am. B* **1986**, *3*, 857.
[37] H. Cao, Y. G. Zhao, S. T. Ho, E. W. Seelig, Q. H. Wang, R. P. H. Chang, *Phys. Rev. Lett.* **1999**, *82*, 2278.
[38] C. W. Cheng, B. Liu, H. Y. Yang, W. W. Zhou, L. Sun, R. Chen, S. F. Yu, J. X. Zhang, H. Gong, H. D. Sun, H. J. Fan, *ACS Nano* **2009**, *3*, 3069.
[39] S. F. Yu, C. Yuen, S. P. Lau, H. W. Lee, *Appl. Phys. Lett.* **2004**, *84*, 3244.
[40] H. Cao, *Waves Random Media* **2003**, *13*, R1.